DOI: 10.1002/ejic.200800108

Solvent-Mediated Ion Exchange and Structural Transformations of Cluster-Based Coordination Polymers

Jian-Jun Zhang,[a] Yue Zhao,[a] Sergio Aarón Gamboa,[a] Miguel Muñoz,[b] and Abdessadek Lachgar*[a]

Keywords: Cluster compounds / Metal *salen* complexes / Coordination polymers / Structural modification / Self-assembly

Reactions between $[Nb_6Cl_{12}(CN)_6]^{4-}$ and $[Mn(salen)]^+$ in MeOH/H_2O solvent mixture led to the formation of $\{[Mn(salen)(H_2O)]_2[(Mn(salen))_2(Nb_6Cl_{12}(CN)_6)]\}\cdot 0.66\,MeOH\cdot 5.33\,H_2O$ (**1**) which has a 2D anionic 4,4′-network built of $[Nb_6Cl_{12}(CN)_6]^{4-}$ and $[Mn(salen)]^+$ nodes linked by CN ligands. The layers in **1** stack perfectly on top of each other and generate channels where dimeric complexes $[Mn(salen)(H_2O)]_2^{2+}$ are located. Unusual cation-induced solvent-mediated structural transformations have been observed when **1** was exposed to solutions of different cations. In contact with $(Me_4N)Cl$ in MeOH, **1** is transformed to the 2D framework of the previously reported compound $[Me_4N]_2[(Mn(salen))_2(Nb_6Cl_{12}(CN)_6)]$ (**2**). In the presence of $(Et_3BzN)^+$, **1** is transformed into a mixture of $[Et_3BzN]_2[(Mn(salen)(MeOH))_2(Nb_6Cl_{12}(CN)_6)]\cdot 4\,MeOH$ (**3**) and $[Et_3BzN]_2[(Mn(salen))_2(Nb_6Cl_{12}(CN)_6)]\cdot 3\,H_2O$ (**4**) which are formed as crystals suitable for single-crystal X-ray diffraction. Compound **3** consists of heterotrimeric supramolecular anions built of $[Nb_6Cl_{12}(CN)_6]^{4-}$ linked to two $[Mn(salen)(H_2O)]^+$ through two CN ligands located in axial positions, while **4** features 2D anionic 4,4′-net with the same connectivity as that observed for **1** and **2** but different layer stacking and interlayer spacing. In contact with methanolic solution of $(Et_4N)^+$, **1** is converted to $[Et_4N]_2[(Mn(salen)(H_2O))_2(Nb_6Cl_{12}(CN)_6)]\cdot 6\,H_2O$ (**5**) which is built of heterotrimeric structural motif similar to those found in **3**. In the presence of M^+ [$M^+ = Li^+$, Na^+, K^+, $(Bu_4N)^+$, or $(PPh_4)^+$], the 2D framework of **1** is transformed to heteropentamers built of $[Nb_6Cl_{12}(CN)_6]^{4-}$ linked to four $[Mn(salen)(MeOH)]^+$: $[(Mn(salen)(MeOH))_4(Nb_6Cl_{12}(CN)_6)]\cdot 4\,MeOH$ (**6**). The mechanism for these unusual solvent-mediated phase-to-phase transformation is discussed.

(© Wiley-VCH Verlag GmbH & Co. KGaA, 69451 Weinheim, Germany, 2008)

Introduction

Hybrid materials and coordination polymers have received much attention in the past decade due primarily to their potential use in heterogeneous catalysis, adsorption and separation.[1] Initial investigations focused on rigid frameworks and evolved toward new generation of flexible frameworks with dynamic structural transformations in response to external stimuli.[2] Most of the reported work has focused on pore-size adjustment and giant structural changes,[3–7] however, only a few of these reports have investigated the mechanistic aspects of dynamic structural transformations.[8] Most transformations are believed to occur through solid-state mechanism with either crystal-to-crystal or amorphous-to-crystal transformations. In most reactions it is believed that the solvent merely acts as a vehicle for guest molecules or ions in the case of ion-exchange reactions. However, Schröder et al. have demonstrated that anion exchange in Ag^I coordination polymers is solvent-mediated and involves slow dissolution of the initial crystalline phase and growth of another phase.[9] Thus, when crystals of Ag^I coordination polymers were immersed in aqueous solutions containing different anions, the crystals do not change size or shape but quickly lose optical transparency and their single crystalline integrity. Transmission electron microscopy (TEM) and atomic force microscopy (AFM) experiments showed the crystals to slowly dissolve when immersed in solvent, and a new crystalline phase grows on the surface of the original phase and the process continues until anion exchange is complete. The complex behavior of coordination polymers in the presence of guest molecules requires more careful investigations that are lacking at the moment. In this paper ion exchange and other structural transformations of cluster-based coordination polymers is shown to occur through cation-induced solvent-mediated mechanism.

Edge-capped $M_6L^i_{12}L^a_6$ (M = Nb, Ta) or face-capped $M_6L^i_8L^a_6$ (M = Mo, W, Re; L = halide, chalcogenide) octahedral metal clusters can be synthesized most conveniently through solid-state reactions.[10] The clusters can subsequently be excised from the solid and can be subjected

[a] Department of Chemistry, Wake Forest University, Winston-Salem, North Carolina 27109, USA
[b] Centro de Investigaciones Quimicas, Universidad Autonoma del Estado de Morelos, Avenue Universidad 1001, Col. Chamilpa, Cuernavaca, Morelos 62210, Mexico

Supporting information for this article is available on the WWW under http://www.eurjic.org or from the author.

 WILEY InterScience DISCOVER SOMETHING GREAT © 2008 Wiley-VCH Verlag GmbH & Co. KGaA, Weinheim

to ligand-substitution reactions leading to the formation of clusters functionalized with different terminal ligands. The function, size, and charge of these clusters can be tailored by judicious choice of ligands. Furthermore, the clusters are characterized by their variety of electronic and magnetic properties arisen from the presence of metal–metal bond within the M_6 octahedral core.[10] The combination of M_6 clusters equipped with suitable bridging ligands and metal complexes with specific geometry, coordination requirement, and functionality has been shown to be a promising method for the preparation of nanomolecular assemblies and hybrid inorganic-organic materials with different dimensions and topologies.[11–16] Compared with mononuclear species, the use of M_6 clusters as nodes is rationalized by their large size (≥1 nm), availability of multiple coordination sites, as well as the potential to create materials with structural features and chemical-physical properties that can be affected by the use of different cluster types and different metals.[11–16]

We have previously reported that depending on the cation used, reactions between $[Nb_6Cl_{12}(CN)_6]^{4-}$ and $[Mn(salen)]^+$ in methanol lead to the formation of either a 2D framework $[Me_4N]_2[(Mn(salen))_2(Nb_6Cl_{12}(CN)_6)]$ (**2**) built of anionic layers formed through CN linkages between $[Nb_6Cl_{12}]^{2+}$ clusters and $[Mn(salen)]^+$, or 3D hydrogen-bonded frameworks based on heterotrimer dianions $[(Mn(salen)(H_2O))_2(Nb_6Cl_{12}(CN)_6)]^{2-}$ connected to each other through hydrogen bonding between coordinated MeOH and CN ligand.[14] The use of MeOH/H_2O as solvent mixture led to the formation of **1** which consists of a 2D anionic framework in which in-situ generated dimeric dications $[Mn_2(L)_2]^{2+}$ act as charge-balancing templates.[15(e)] Herein we report on the reactivity of **1** in the presence of solutions containing different cations. The findings indicate that **1** undergoes solvent-mediated ion-exchange reactions and structural transformation. A possible mechanism for these chemical and structural transformations is proposed.

Results and Discussion

Structure of the $[Nb_6Cl_{12}(CN)_6]^{4-}$ Building Unit

The structures of all four compounds contain the same $[Nb_6Cl_{12}(CN)_6]^{4-}$ cluster unit, which is characterized by its octahedral Nb_6 metal core with 12 edge-bridging Cl ligands and six terminal CN^- ligands connected to the cluster through their carbon end. A comparison of the most important bond lengths and angles of the compounds are listed in Table 1. The bond lengths and angles of Nb–Nb, Nb–Cl, Nb–C, C≡N and Nb–C≡N are close to the corresponding values reported for other compounds containing 16e octahedral cyanochloride niobium cluster units.[14,15] The IR C≡N stretching bands are near 2130 cm^{-1} close to that found for the starting material $(Me_4N)_4[Nb_6Cl_{12}(CN)_6]$ (2129 cm^{-1}).[14]

Two-Dimensional Frameworks of 1, 2 and 4

The three compounds feature similar two-dimensional 4,4′-network with $[Mn(salen)(H_2O)]_2^{2+}$, $[Me_4N]^+$ and

Table 1. Important bond lengths [Å] and angles [°] for some $\{Nb_6\}$–Mn(*salen*) compounds.

	1	**2**[a]	**4**	**5**	**6**	**A**[a]	**B**[b]
Nb–Nb (mean)	2.9320(8)	2.924(6)	2.928(2)	2.931(1)	2.9304(6)	2.934(6)	2.927(4)
Nb–Cl (mean)	2.4686(1)	2.460(8)	2.462(4)	2.462(2)	2.462(1)	2.465(8)	2.464(7)
Nb–C[c]	2.291(5)	2.273(4)	2.271(15)	2.281(9), 2.261(9)	2.283(5)	2.274(4), 2.283(4)	2.282(7), 2.283(5)
Nb–C[d]	2.275(5) 2.285(5)	2.286(4), 2.277(4)	2.275(17), 2.282(11)	2.282(8)	2.302(4) 2.287(4)	2.302(4)	–
C≡N (non-bridging)	1.152(6)	1.131(5)	1.116(18)	1.132(10), 1.147(11)	1.138(6)	1.141(5), 1.146(5)	1.134(9), 1.126(6)
C≡N (bridging)	1.142(5), 1.145(6)	1.131(4), 1.137(4)	1.166(17), 1.149(18)	1.153(10)	1.139(5) 1.141(5)	1.143(5)	–
Cl–Nb–Cl (mean)	88.74(4)	88.67(3)	88.8(1)	88.75(7)	88.75(4)	88.76(3)	88.61(6)
Nb–Nb–Nb (mean)	90.00(2)	90.00(1)	90.00(5)	90.00(3)	90.00(1)	90.00(1)	89.98(2)
C–Nb–Cl (mean)	81.5(1)	81.4(1)	81.5(4)	81.53(2)	80.7(1)	81.5(1)	81.5(2)
Nb–Cl–Nb (mean)	72.93(3)	72.98(3)	73.1(1)	73.04(5)	73.03(3)	73.06(2)	72.86(5)
Nb–C≡N (non-bridging)	176.9(4)	175.3(4)	175(2)	179.5(9), 176.7(8)	175.2(4) 172.7(4)	177.2(4), 176.1(4)	178.6(6), 177.8(7)
Nb–C≡N (bridging)	177.0(4), 174.9(4)	174.7(3), 175.2(3)	173.1(14), 176.2(15)	175.4(7)	177.7(5)	176.8(3)	–
Mn–N_{CN}	2.293(4), 2.321(4)	2.233(3), 2.365(3)	2.349(14), 2.328(14)	2.284(7)	2.243(4) 2.293(4)	2.295(3)	–
Mn–$O_{solvent}$	2.187(4)	–	–	2.316(5)	2.404(3) 2.313(3)	2.320(3)	–
C≡N–Mn	147.3(3), 150.0(4)	155.0(3), 144.2(3)	149.1(13), 144.4(13)	161.4(7)	161.3(4) 149.5(3)	157.2(3)	–
N_{CN}–Mn–N_{CN}	166.39(14)	173.33(12)	164.6(4)	–	–	–	–

[a] A is $[Et_4N]_2[(Mn(salen)(MeOH))_2(Nb_6Cl_{12}(CN)_6)]\cdot 2\,MeOH$, data from ref.[14] [b] B is the starting material $(Me_4N)_4[Nb_6Cl_{12}(CN)_6]$, data from ref.[14] [c] Carbon from non-bridging cyanide ligand. [d] Carbon from bridging CN ligand.

 © 2008 Wiley-VCH Verlag GmbH & Co. KGaA, Weinheim

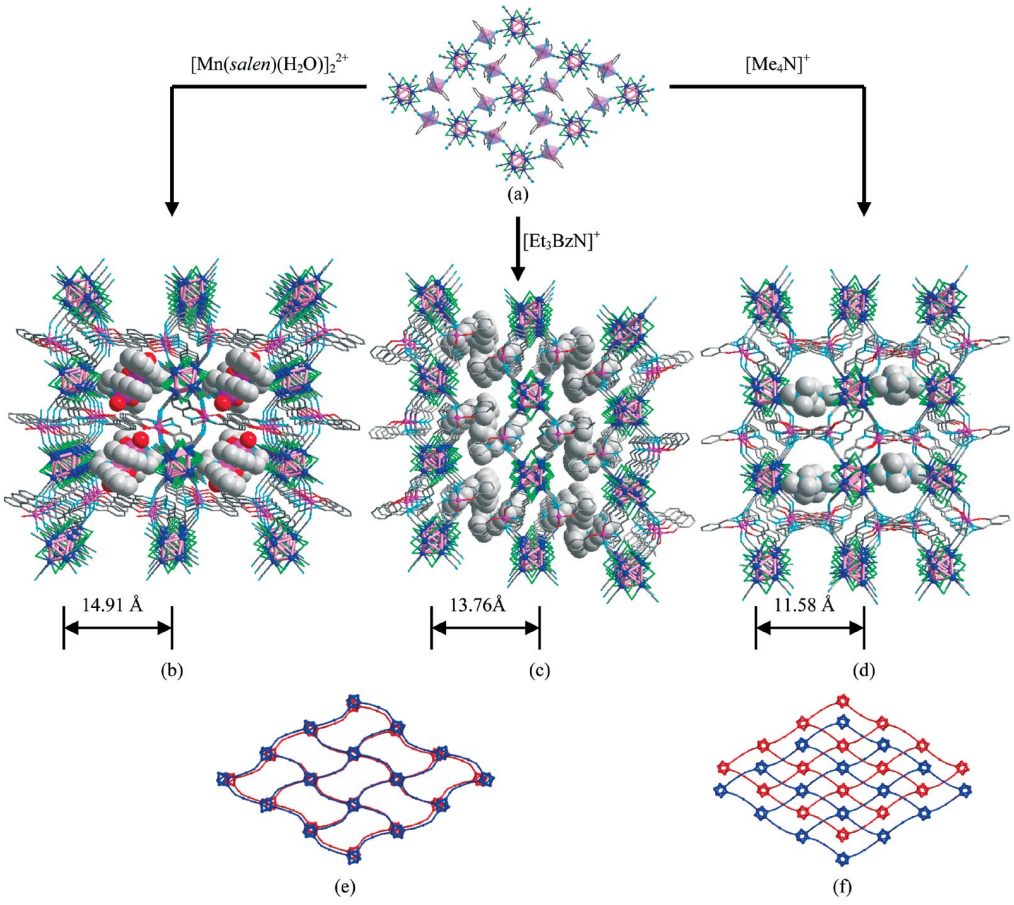

Figure 1. (a) The structure of the 2D anionic 4,4-network. (b) The packing diagram of **1**. (c) The packing diagram of **4**. (d) The packing diagram of **2**. (e) The perfectly stacked packing mode of the layers in **1** and **4**. (f) The staggered arrangement of the layers in **2**. The *salen* ligands and Cl atoms are omitted for clarity in (e) and (f). The diagrams in (a), (e) and (f) are viewed along the *a* direction while in (b), (c) and (d) the crystal structure is viewed along the *b* direction.

$[Et_3BzN]^+$ as cations, respectively (Figure 1). The anionic layer is built of $[Nb_6Cl_{12}(CN)_6]^{4-}$ nodes that use four of their six cyanide ligands to connect to four different Mn^{III} complexes, and each manganese complex connects two clusters through cyanide bridges.

The four $[Mn(salen)]^+$ complexes are all located in the equatorial plane of the octahedral cluster. Each Mn^{3+} ion has a distorted octahedral coordination environment that consists of two N and two O from the tetradentate *salen* ligand with bond lengths Mn–O 1.893(3) Å and Mn–N 1.995(4) Å for **1**; Mn–O 1.878(3) Å and Mn–N 1.99(2) Å for **2**; Mn–O 1.86(1) Å and Mn–N 1.96(1) Å for **4**, compared with Mn–O 1.882(1) Å and Mn–N 1.983(1) Å in the precursor $[Mn(salen)Cl(H_2O)]$;[17] and two N from bridging cyanide ligands with $Mn–N_{CN}$ bond lengths between 2.233(4) and 2.365(3) Å. The $[Mn(salen)]^+$ complexes are linked to the cluster node in axial positions with C≡N–Mn angles between 144.2(3) and 155.0(3)°. The 2D nets in **1**, **2** and **4** are direct expansion of the network of $(Et_4N)_2[Mn(salen)_2Fe(CN)_6]$ in which $[Fe(CN)_6]^{4-}$ takes the place of the cluster $[Nb_6Cl_{12}(CN)_6]^{4-}$.[18]

Although the frameworks in the three compounds are built from the same building blocks and have same connectivity, there are some differences between them (Table 2). First, depending on the counterion, the 2D network is distorted differently, and the $N_{CN}–Mn–N_{CN}$ angles are significantly different (166.4, 173.3, 164.6° for **1**, **2** and **4**, respectively). The manganese ions are found at different distances from the plane defined by the centers of clusters within the

Table 2. Comparison of the three 4,4′-nets in **1**, **2** and **4**.

	1	**2**	**4**
Cluster···cluster[a]	13.19	13.30,13.01	13.02
Mn···cluster	7.51	7.51; 7.44	7.54; 7.51
∠Cluster–Mn–cluster	122.71	125.59	119.77
Mn···plane[b]	3.04	3.30	3.76
Angle[c]	50.94	52.14	60.27
Angle[d]	17.3	34.9	15.6
$\angle N_{CN}–Mn–N_{CN}$	166.4	173.3	164.6
Layers distance	14.91	11.58	13.76
Effective free vol.[e] [Å^3]	539.7/11.9%	590.0/8.4%	251.0/6.2%

[a] The separation is defined as the distance between the centers of the clusters. [b] The plane is defined by the centers of the clusters within the same layer. [c] Angle between the plane and a line defined by the non-bridging cyanide ligand (cluster tilting). [d] Dihedral angle between the two benzene rings of *salen* ligand. [e] Free solvent not included.

 © 2008 Wiley-VCH Verlag GmbH & Co. KGaA, Weinheim

same layer: 3.04, 3.30, 3.76 Å for **1**, **2** and **4**, respectively, yet the Mn^{3+}···cluster separations are all close to 7.5 Å in the three nets. Second, the *salen* ligand is significantly more distorted in **2** compared to **1** and **4**. The dihedral angle between the two benzene rings of the *salen* ligand in **2** (34.9°) is markedly different from that in **1** (17.3°) and in **4** (15.6°). This distortion is probably due to halide-π electron donor-acceptor charge-transfer interaction between the edge-bridging Cl ligand and the benzene ring of *salen* ligand as indicated by the remarkably short distances of 3.25 Å between Cl and the benzene ring. The halides-arenes interactions are well documented.[19] Third, the clusters' tilt with respect to the median plane of the layer is different in the three compounds. The angle measured between a line containing the two non-bridging cyanide ligands and the plane defined by the centers of the clusters is 50.94, 52.14 and 60.27° for **1**, **2** and **4**, respectively.

Compound **1** uses the dimer $[Mn(salen)(H_2O)]_2^{2+}$ as charge compensating cation while **2** and **4** use $(Me_4N)^+$ and $[Et_3BzN]^+$, respectively. Each Mn^{3+} in the dimer is chelated by 2N and 2O from the tetradentate *salen* ligand, and an aqua ligand with Mn–O 2.187(4) Å. The two Mn^{3+} are linked together by phenolic oxygen atoms which complete their octahedral coordination environment [Mn–O 2.977(4) Å]. The Mn···Mn separation and Mn–O–Mn angle are 3.571(1) Å and 92.1(1)°, respectively, within the range reported for other Mn(*salen*)-type dimers (3.19–4.38 Å and 91.1–102.4°, respectively).[20] The formation of the dimers results from the offset face-to-face π–π interactions between the benzene rings of the *salen* ligands in the two manganese complexes with shortest distance being 3.32 Å. The dimers further interact with the *salen* ligands from the Mn complexes within the layers through another offset face-to-face π–π interactions with distances of 3.48 and 3.68 Å leading to formation of 1D π–π stacking running along the crystallographic *c* direction. This π–π interactions help stabilize the framework together with hydrogen-bond interactions between the coordinated water molecules and non-bridging cyanide ligands with O···N separation of 2.876(5) Å and O–H···N angle of 172.45(4)°. The layers are staked perfectly on top of each other to generate channels along the *a* axis where the dimeric cations and solvent molecules are located. In **2**, no strong interactions are found between the $(Me_4N)^+$ cations and the framework. In **4**, The closest contact between the benzene ring of the $[Et_3BzN]^+$ cation and the *salen* ligand is H_{52B}-ring 2.82, indicating relatively strong edge-to-face π–π interactions.

The cations have a significant effect on the layers' stacking and interlayer spacing (Table 2). In **1** and **4**, the layers stack perfectly on top of each other along the *a* direction while in **2** the layers are stacked in a staggered fashion. When $[Mn(salen)(H_2O)]_2^{2+}$ is exchanged for the smaller cation $[Et_3BzN]^+$ the interlayer spacing is decreased from 14.91 Å to 13.76 Å). While substitution of the dimeric cation by $[Me_4N]^+$ leads to a decrease from 14.91 Å to 11.58 Å in the interlayer spacing and a shift of 6.7 Å between neighboring layers along the *b* direction. The cations also have a significant effect on the total effective free volume which is found to be 539.7, 590.0 and 251.0 $Å^3$ for **1**, **2** and **4**, respectively, comprising 11.9, 8.4 and 6.2% of the crystal volume, as calculated by the program PLATON.[21] In **2**, only $[Me_4N]^+$ cations are captured in the channel, while in **1** and **4** both cations ($[Mn(salen)(H_2O)]_2^{2+}$ or $[Et_3BzN]^+$) and solvent molecules are present in the channel.

Structure of 5 and 3

The crystal structure of **5** can be described as cation-assisted hydrogen-bonded 3D framework built of dianionic heterotrimers formed of $[Nb_6Cl_{12}(CN)_6]^{4-}$ linked to two $[Mn(salen)]^+$ by cyanide ligands located on oposite sides of

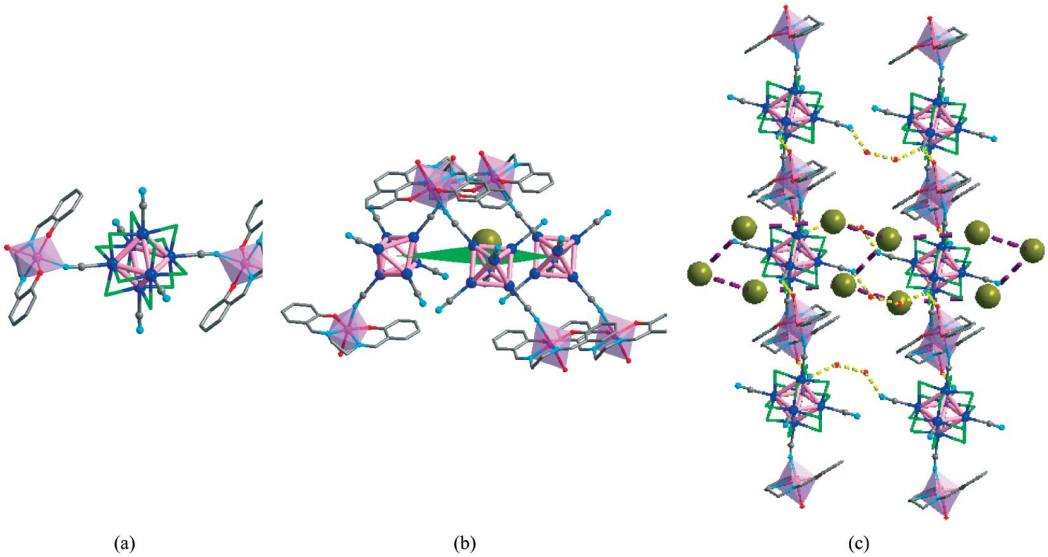

Figure 2. (a) The structure of the heterotrimer building block in **5**. (b) The environment of the cation $[Et_4N]^+$. (c) The hydrogen-bonded networks and the environment of the heterotrimers. $[Et_4N]^+$ cations are represented as large grey spheres.

 © 2008 Wiley-VCH Verlag GmbH & Co. KGaA, Weinheim

the cluster with ∠C≡N–Mn 161.5(7)° (Figure 2). The octahedral coordination environment of manganese is completed by an aqua ligand that form hydrogen bonds with non-bridging cyanide ligands from neighboring trimers (O3···N102 2.89 Å) to form 1D hydrogen-bonded double chains that pack along the crystallographic *a* axis. Free water molecules connect the chains first into layers (N102···O12 2.80 Å; O12···O11 2.86 Å; O11···N103 2.86 Å) then into 3D hydrogen-bonded framework (O11···O3 2.75 Å) with cavities where the cations $(Et_4N)^+$ are located. Each heterotrimer is surrounded by six $(Et_4N)^+$ cations that form a hexagonal ring with side length of 7.27–7.92 Å while each cation is surrounded by three trimers that form a triangle with side length of ~11.5 Å. Except for the solvent molecules, the structure of **5** is similar to that of $[Et_4N]_2[(Mn(salen)(MeOH))_2(Nb_6Cl_{12}(CN)_6)]\cdot 2\,MeOH$ obtained by direct mixing of $(Et_4N)_4[Nb_6Cl_{12}(CN)_6]$ and [Mn(*salen*)]ClO_4 in MeOH.[14]

Only low X-ray quality crystals of **3** could be obtained (weak intensity reflections and twinning) which prevented good and complete structural characterization. Nevertheless, the best data obtained was indexed to give a triclinic unit cell, space group *P*1 with a = 13.051(2), b = 13.514(2), c = 14.863(2) Å, α = 112.74(0), β = 106.33(0), γ = 95.42(0)°, V = 2258(3) Å^3. The overall structure of **3** was determined to be built of heterotrimers similar to those found in **5** that are terminated by coordinated methanol molecules. The cation $[Et_3BzN]^+$ acts as counterion.

$[(Mn(salen)(MeOH))_4(Nb_6Cl_{12}(CN)_6)]\cdot 4\,MeOH$ (6)

Crystal structure analysis shows that in **6**, the octahedral cluster is linked to four $[Mn(salen)(MeOH)]^+$ complexes through four cyanide ligands from the equatorial plane with C≡N–Mn angles of 149.5(3) and 161.3(4)° (Figure 3). Adjacent heteropentamers are linked to each other by hydrogen bonding between the N end of non-bridging cyanide ligands and MeOH ligands [N103···O11 2.714(6) Å, ∠O11–H11B···N103 173(6)°] to form hydrogen-bonded double chains running along the *a* direction (Figure 3). The chains are further connected through hydrogen bonds between the MeOH ligand (O11 and O12) and MeOH solvent molecule (O13) [O11···O13 2.872(6) Å, O13–H13C···O11 162(7)°; O13···O12 2.695(5) Å, O12–H12B···O13 168(6)°] to form 2D hydrogen-bonded frameworks with channels where free methanol molecules (neither coordinated nor hydrogen-bonded to other molecules) are located.

Synthesis and Cation-Induced Transformations

We have previously reported that reaction between $(Me_4N)_4[Nb_6Cl_{12}(CN)_6]$ and $[Mn(salen)]^+$ in pure methanol leads to formation of the 2D compound **2**: $[Me_4N]_2[(Mn(salen))_2(Nb_6Cl_{12}(CN)_6)]$.[14] When the same reaction is carried out in a mixture of methanol and water as solvent a new compound which bears similar 2D net but with dimeric complexes $[Mn(salen)(H_2O)]_2^{2+}$ as charge compensating ions is formed. Solvent-mediated structural transformations schematically presented in Scheme 1, have been observed when **1** was exposed to solutions containing different cations.

(A) When crystals of **1** are left in a solution containing excess $[Me_4N]Cl$ in methanol, the phase is irreversibly transformed into the 2D framework of the previously reported compound **2** with $(Me_4N)^+$ as cation. The transformation is complete as indicated by PXRD, elemental analysis and IR.

(B) In contact with a saturated solution of $[Et_3BzN]Cl$ a mixture containing compounds **3** (heterotrimer) and **4** (2D framework), both using $[Et_3BzN]^+$ as cations, was obtained as single crystals.

(C) In the presence of excess $[Et_4N]^+$ in methanol, the heterotrimer **5**, whose structure is almost the same as that

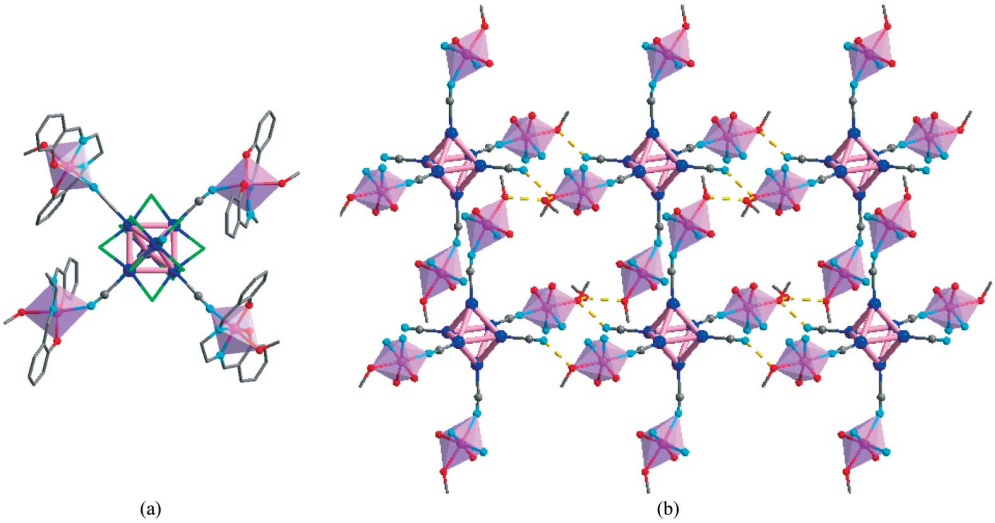

Figure 3. (a) The neutral heteropentamer in **6**. (b) The hydrogen-bonded networks in **6**; *salen* ligand and chlorine atoms are omitted for clarity. Hydrogen bond is represented as dotted lines.

 © 2008 Wiley-VCH Verlag GmbH & Co. KGaA, Weinheim

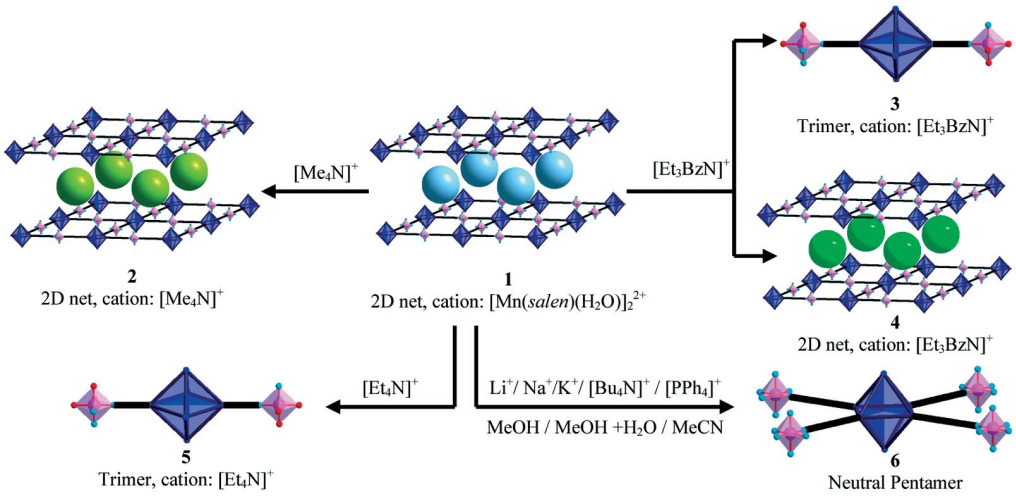

Scheme 1. A summary of all solvent-mediated structural transformations observed in this study.

obtained through direct reaction of $(Et_4N)_4[Nb_6Cl_{12}(CN)_6]$ and $[Mn(salen)]^+$ in methanol,[14] was obtained.

(D) When **1** was exposed to a solution containing a mixture of cations, either $[Me_4N]^+$ and $[Et_4N]^+$, or $[Me_4N]^+$ and $[Et_3BzN^+]$ only **2** was obtained which indicates that the reaction is cation specific most likely due to lower solubility of compound **2** compared to the other phases.

(E) In methanol solutions containing Li^+ (or Na^+, K^+, $[Bu_4N]^+$, $[PPh_4]^+$), or in the absence of any foreign species (neat solvents) [either MeOH, or (MeOH + H_2O), or MeCN], only the heteropentamer **6** was obtained.

Two observations indicate that these transformations are solvent-mediated: i) the mixtures remained as suspensions rather than transparent solutions throughout the transformation process, and ii) **1** remains stable when left in THF for more than a week or exposed in 100% humidity for more than a month. As the product phase is formed, the solubility equilibrium is shifted toward the product until complete transformation of the precursor. The change in $[Mn(salen)]^+/\{Nb_6\}$ ratio between the precursor **1** (4:1) and the products **2**, **3**, **4** or **5** (2:1) strongly suggests the involvement of an intermediate with $[Mn(salen)]^+/\{Nb_6\}$ ratio of 2:1. Thus a possible mechanism of these reactions can be suggested as follows: In methanol, compound **1** dissociates slowly to form the dimer $[Mn(salen)(H_2O)]_2^{2+}$ and the heterotrimer $[Mn(salen)_2(Nb_6Cl_{12}(CN)_6)]^{2-}$. In the presence of excess suitable cation, the heterotrimers reassemble to form 2D frameworks of either **2** ($[Me_4N]^+$) or **4** ($[Et_3BzN]^+$). In excess $[Et_3BzN]^+$ or $[Et_4N]^+$, the 0D heterotrimer crystallizes directly as compounds **3** and **5**. The cation $[Et_3BzN]^+$ is interesting in that it can yield either the heterotrimer or 2D 4, 4′-net. In the absence of suitable cations, the heterotrimer captures the $[Mn(salen)]^+$ species present in solution to form neutral heteropentamer **6**.

Materials with 4,4′-network connectivity are among the most dynamically flexible frameworks that can undergo changes caused by external stimuli, either within the layers or between them.[22,23] Thus, the reverse transformation of the edge-to-edge regular packing mode and the staggered packing mode can be triggered by guest exchange.[24] The transformation of **1** to **2** and **4** are cation-exchange processes. Yet only certain cations can stabilize the 4,4′-net. $[Mn(salen)]_2^{2+}$ and $(Et_3BzN)^+$ can be captured because their weak interactions with 4,4′-net such as π–π and/or hydrogen bonds help stabilize the structures. The stability of **2** can be attributed to its lack of solubility in methanol and its thermodynamic stability.

Although most reports refer to solid-state and sometimes even crystal to crystal mechanism for ion-exchange processes and structural transformation in dynamic coordination polymers,[4–8] solvent-mediated ion-exchange processes involving dissolution of one crystalline phase and crystallization of a new phase in the presence of new anions were observed in Ag-based coordination polymers even though the number, size and shape of the crystals remain the same after the guest exchange reactions.[9,25] The findings here are compatible with Schröders' study with the major difference being that in the present study the original framework is regenerated only for specific cations. Perhaps that the most interesting outcome of the current study is that solvent-mediated structural transformations can be used to develop methodologies for the crystallization of compounds that cannot be directly (or easily) obtained by direct mixing of their molecular components. The key then will be to identify and prepare precursors that can serve as a source of well defined molecular intermediate components that can be released in a slow fashion. A case in point is the fact that it was not possible to synthesize compound **5** by directly mixing $[Mn(salen)]ClO_4{\cdot}2H_2O$ and $(Et_3BzN)_4[Nb_6Cl_{12}(CN)_6]$ in MeOH or MeOH/H_2O. The product was found to be amorphous to X-rays as confirmed by PXRD. Even more important was the preparation of the compound $\{[Mn(salen)(MeOH)]_2(dpyo)\}$ $\{(dpyo)[(Mn(salen))_2Nb_6Cl_{12}(CN)_6]\}dpyo$ which has 1D coordination framework built of heterotrimer intermediates connected to each other by 4, 4′-dipyridyl *N*,*N*′-dioxide (*dpyo*) ligands when **1** was left in a methanol solution containing excess *dpyo*.[15(e)]

 © 2008 Wiley-VCH Verlag GmbH & Co. KGaA, Weinheim

Conclusions

A 2D cluster-based coordination polymer with 4,4′-net was assembled in a MeOH/H_2O solvent mixture using the metal-ligand-directed assembly methodology. Its chemical reactivity in solutions containing different cations has shown that depending on the cation present in solution either solvent-mediated ion-exchange reactions or structural transformations occur. This work, together with that of Schröder confirm that ion-exchange in coordination polymers can indeed be solvent-mediated. While solid-state mechanism is obviously true for some transformations, it is not the case for all transformations including ion-exchange reactions. For those transformations involving the presence of solvent, one cannot conclude that they occur through solid-state mechanism based on the conservation of the framework, even when the number, shape and size of crystals remain the same. The solvent-mediated structural transformation reactions described here may allow for the development of synthesis methodology for the assembly of materials not directly (or easily) accessible via direct mixing of their molecular components.

Experimental Section

General: $(Me_4N)_4[Nb_6Cl_{12}(CN)_6]\cdot 2MeOH$ and [Mn(*salen*)]$ClO_4\cdot 2H_2O$ were synthesized according to literature methods.[14,26] LiCl (99%), $NbCl_5$ (99%, metal basis), Nb powder (99.8%, metal basis), KCN (96%), Me_4NCl (98%) and $(Bu_4N)Br$ (99%) were purchased from Alfa Aesar. $Mn(OAc)_3\cdot 2H_2O$ (98%) and ethylenediamine (99%) were purchased from ACROS. $(Et_3BzN)Cl$ (99%), PPh_4Br (97%), and $(Et_4N)Br$ (99%) were purchased from Aldrich. NaCl, KSCN, salicylaldehyde were purchased from Fisher. All chemicals were used as received. The solvents EtOH, THF, MeCN and MeOH were used as received without further purification.

{[Mn(*salen*)(H_2O)]$_2$[(Mn(*salen*))$_2$($Nb_6Cl_{12}(CN)_6$)]}·0.66 MeOH·5.33 H_2O (1): To 10.0 mL of 12.0 mM solution of [Mn(*salen*)]$ClO_4\cdot 2H_2O$ in methanol was added 10.0 mL of 4.0 mM aqueous solution of $(Me_4N)_4[Nb_6Cl_{12}(CN)_6]\cdot 2MeOH$. Brown microcrystalline precipitate formed immediately. The resulting mixture was kept stirring for 30 min and the solid was collected by centrifugation washed with MeOH then dried under vacuum for 20 min (Yield: 18.7 mg, 25%). Brown hexagonal plate-like crystals suitable for X-ray analysis were obtained by layering the methanolic solution of 1.0 mL of the complex solution onto 1.0 mL of an aqueous solution of the cluster. $C_{70.67}H_{73.33}Cl_{12}Mn_4N_{14}Nb_6O_{16}$ (2577.36): calcd. C 32.93, H 2.87; found C 32.73, H 2.70. IR: ν_{CN} = 2131 cm^{-1}.

Solvent-Mediated Structural Transformation: The procedure of a typical reaction is outlined: $(Me_4N)Cl$ (100 mg, 0.9 mmol) was added to a suspension of microcrystalline **1** (26 mg, 0.01 mmol) in methanol (10 mL) at room temperature. The reaction mixture was left undisturbed for 2 d after which the solid was separated by centrifugation, washed with water and methanol, then dried in vacuo to get $[Me_4N]_2$[(Mn(*salen*))$_2$($Nb_6Cl_{12}(CN)_6$)] (**2**). $C_{46}H_{52}Cl_{12}Mn_2N_{12}Nb_6O_4$ (1929.75): calcd. C 28.63, H 2.78, N 8.31; found C 28.79, H 2.87, N 8.23. Compounds $[Et_3BzN]_2$-[(Mn(*salen*)(MeOH))$_2$($Nb_6Cl_{12}(CN)_6$)]·4 MeOH (**3**) and $[Et_3BzN]_2$-[(Mn(*salen*))$_2$ ($Nb_6Cl_{12}(CN)_6$)]·3 H_2O (**4**) were prepared as a mixture by reaction of **1** in methanolic solution of $(Et_3BzN)Cl$. Compound $[Et_4N]_2$[(Mn(*salen*)(H_2O))$_2$($Nb_6Cl_{12}(CN)_6$)]·6H_2O (**5**) was prepared by the reaction between **1** and $(Et_4N)Cl$. Compound [(Mn(*salen*)(MeOH))$_4$($Nb_6Cl_{12}(CN)_6$)]·4MeOH (**6**) was obtained by soaking **1** in methanol. Single crystals of **3**, **4**, **5** and **6** suitable for X-ray structural analyses were also prepared by this method. All the products were characterized by single crystal and powder XRD, and IR absorption spectroscopy.

Compound 3: $C_{70}H_{96}Cl_{12}Mn_2N_{12}Nb_6O_{10}$ (2358.36): calcd. C 35.65, H 4.10, N 7.13.

Compound 4: $C_{64}H_{72}Cl_{12}Mn_2N_{12}Nb_6O_7$ (2214.08): calcd. C 34.72, H 3.28, N 7.59; found C 34.74, H 3.41, N 7.27.

Compound 5: $C_{54}H_{80}Cl_{12}Mn_2N_{12}Nb_6O_{10}$ (2150.04): calcd. C 30.10, H 3.79, N 7.65; found C 30.27, H 3.77, N 7.77.

Table 3. Crystal data and structure refinement for the complexes.

	1	**4**	**5**	**6**
Formula	$C_{70.67}H_{73.33}Cl_{12}Mn_4N_{14}Nb_6O_{16}$	$C_{64}H_{72}Cl_{12}Mn_2N_{12}Nb_6O_7$	$C_{54}H_{80}Cl_{12}Mn_2N_{12}Nb_6O_{10}$	$C_{78}H_{88}Cl_{12}Mn_4N_{14}Nb_6O_{16}$
M [g mol^{-1}]	2577.36	2214.08	2150.04	2582.25
Crystal system	monoclinic	monoclinic	monoclinic	monoclinic
Space group	$P2_1/c$	$P2_1/c$	$P2_1/c$	$P2_1/n$
a [Å]	14.949(4)	13.960(2)	13.381(2)	13.9497(17)
b [Å]	13.373(4)	13.033(2)	20.966(4)	12.8984(15)
c [Å]	22.736(6)	22.548(4)	13.915(2)	27.432(3)
α [deg]	90	90	90	90
β [deg]	94.409(4)	99.825(3)	91.546(3)	96.004(2)
γ [deg]	90	90	90	90
V [Å^3]/Z	4532(2)/2	4042.4(11)/2	3902.4(12)/2	4909(1)/2
$d_{calcd.}$ [g/cm^3]	1.889	1.819	1.830	1.813
F(000)	2547	2192	2136	2664
θ Range [°]	3.84–27.50	3.80–24.15	3.80–26.00	3.78–27.48
Reflections collected/unique	39497/10382	26900/6406	30471/7643	42828/11193
R(int)	0.0709	0.2026	0.0562	0.0645
Goodness-of-fit on F^2	1.056	1.024	1.206	1.027
$R1$,[a] wR_2[b]				
$I > 2\sigma$ (I)	R_1 = 0.047, wR_2 = 0.095	R_1 = 0.091, wR_2 = 0.18	R_1 = 0.071, wR_2 = 0.148	R_1 = 0.048, wR_2 = 0.097
All data	R_1 = 0.067, wR_2 = 0.103	R_1 = 0.163, wR_2 = 0.197	R_1 = 0.087, wR_2 = 0.15	R_1 = 0.066, wR_2 = 0.105

[a] $R_1 = \Sigma(||F_o| - |F_c||)/\Sigma|F_o|$. [b] $wR_2 = \{\Sigma w[(F^2_oF^2_c)]/\Sigma w[(F^2_o)^2]\}^{0.5}$, $w = [\sigma^2(F^2_o) + (aP)^2 + bP]^{-1}$, where $P = (F^2_o + 2F^2_c)/3$. **1**: a = 0.0358, b = 3.6862; **4**: a = 0.0710, b = 0.0000; **5**: a = 0.0526, b = 20.6193; **6**: a = 0.0488, b = 4.4476.

 © 2008 Wiley-VCH Verlag GmbH & Co. KGaA, Weinheim

Compound 6: $C_{78}H_{88}Cl_{12}Mn_4N_{14}Nb_6O_{16}$ (2582.25): calcd. C 34.95, H 3.31, N 7.32; found C 34.98, H 3.62, N 7.89.

Structural Determination: Intensity data for all compounds were measured at 193(2) K with a Bruker SMART APEX CCD area detector system. Data were corrected for absorption effects using the multi-scan technique (SADABS). All structures were solved and refined using the Bruker SHELXTL (Version 6.1) Software Package. A summary of the most important crystal and structure refinement data for all compounds is given in Table 3.

CCDC-644473 (for **1**), -644474 (for **5**), -675688 (for **4**), -675689 (for **6**) contain the supplementary crystallographic data for this paper. These data can be obtained free of charge from The Cambridge Crystallographic Data Centre via www.ccdc.cam.ac.uk/data_request/cif.

Other Physical Measurements: Elemental analyses were carried out by Atlantic Microlab, Inc. Infrared spectra were recorded as KBr pellets with a Mattson Infinity System FTIR spectrometer. X-ray powder diffraction data was collected at room temperature using a Bruker P4 general-purpose four-circle X-ray diffractometer equipped with a GADDS/Hi-Star detector positioned 20 cm from the sample. The goniometer was controlled using the GADDS software suite.[27] The sample was mounted on tape and data was recorded in transmission mode. The data was reduced by area integration methods to produce a single powder diffraction pattern for each frame. Individual powder diffraction patterns were merged and analyzed with the program EVA to produce a single one-dimensional pattern.[28]

Supporting Information (see footnote on the first page of this article): Detailed description of crystal structure analysis, tables of bond lengths and angles, IR spectra, and PXRD patterns.

Acknowledgments

This material is based upon work supported by the National Science Foundation (Grant No. DMR-0446763).

[1] a) J. M. Lehn, *Supramolecular Chemistry*, VCH, Weinheim, **1995**; b) R. Robson in *Comprehensive Supramolecular Chemistry*, vol. 6 (Eds.: J. L. Atwood, J. E. D. Davies, D. D. MacNicol, F. Vögtle, F. Toda, R. Bishop), Pergamon, Oxford, **1996**, 733–755; c) M. D. Eddaoudi, B. Moler, H. Li, B. Chen, M. O'Keeffe, O. M. Yaghi, *Acc. Chem. Res.* **2001**, *34*, 319–330.

[2] a) S. Kitagawa, R. Kitaura, S. Noro, *Angew. Chem. Int. Ed.* **2004**, *43*, 2334–2375; b) S. Kitagawa, K. Uemura, *Chem. Soc. Rev.* **2005**, *34*, 109–119.

[3] a) X. B. Zhao, B. Xiao, A. J. Fletcher, K. M. Thomas, D. Bradshaw, M. J. Rosseinsk, *Science* **2004**, *306*, 1012–1015; b) R. Kitaura, K. Seki, G. Akiyama, S. Kitagawa, *Angew. Chem. Int. Ed.* **2003**, *42*, 428–431; c) S. Takamizawa, E. Nakata, H. Yokoyama, K. Mochizuki, W. Mori, *Angew. Chem. Int. Ed.* **2003**, *42*, 4331–4334; d) S. Bourrelly, P. L. Llewellyn, C. Serre, F. Millange, T. Loiseau, G. Ferey, *J. Am. Chem. Soc.* **2005**, *127*, 13519–13521.

[4] a) D. N. Dybtsev, H. Chun, K. Kim, *Angew. Chem. Int. Ed.* **2004**, *43*, 5033–5036; b) K. Biradha, M. Fujita, *Angew. Chem. Int. Ed.* **2002**, *41*, 3392–3395; c) K. Uemura, S. Kitagawa, K. Fukui, K. Saito, *J. Am. Chem. Soc.* **2004**, *126*, 3817–3828; d) M. H. Zeng, X. L. Feng, X. M. Chen, *Dalton Trans.* **2004**, 2217–2223; e) H. J. Choi, M. P. Suh, *J. Am. Chem. Soc.* **2004**, *126*, 15844–15851.

[5] a) R. Matsuda, R. Kitaura, S. Kitagawa, Y. Kubota, T. C. Kobayashi, S. Horike, M. Takata, *J. Am. Chem. Soc.* **2004**, *126*, 14063–14070; b) G. J. Halder, C. J. Kepert, B. Moubaraki, K. S. Murray, J. D. Cashion, *Science* **2002**, *298*, 1762–1765.

[6] a) N. Casellas, P. Gamez, J. Reedijk, I. Mutikainen, U. Turpeinen, N. Masciocchi, S. Galli, A. Sironi, *Inorg. Chem.* **2005**, *44*, 7918–7924; b) E. Y. Lee, M. P. Suh, *Angew. Chem. Int. Ed.* **2004**, *43*, 2798–2801; c) A. Cingolani, S. Galli, N. Masciocchi, L. Pandolfo, C. Pettinari, A. Sironi, *J. Am. Chem. Soc.* **2005**, *127*, 6144–6145.

[7] a) A. Kondo, H. Noguchi, S. Ohnishi, H. Kajiro, A. Tohdoh, Y. Hattori, W. C. Xu, H. Tanaka, H. Kanoh, K. Kaneko, *Nano Lett.* **2006**, *6*, 2581–2584; b) T. K. Maji, G. Mostafa, R. Matsuda, S. Kitagawa, *J. Am. Chem. Soc.* **2005**, *127*, 17152–17153.

[8] a) O. M. Yaghi, H. Li, C. Davis, D. Richardson, T. L. Groy, *Acc. Chem. Res.* **1998**, *31*, 474–484; b) K. S. Min, M. P. Suh, *J. Am. Chem. Soc.* **2000**, *122*, 6834–6840; c) O. S. Jung, Y. J. Kim, Y. A. Lee, J. K. Park, H. K. Chae, *J. Am. Chem. Soc.* **2000**, *122*, 9921–9925.

[9] A. N. Khlobystov, N. R. Champness, C. J. Roberts, S. J. B. Tendler, C. Thompson, M. Schröder, *CrystEngComm* **2002**, *4*, 426–431.

[10] a) F. A. Cotton, R. A. Walton, *Multiple bonds between metal atoms*, 2. ed., Oxford University Press, **1993**; b) U. Kreibig, M. Vollmer, *Optical properties of metal clusters*, Springer-Verlag, **1995**; c) E. J. Welch, J. R. Long, *Prog. Inorg. Chem.* **2005**, *54*, 1–45; d) J.-C. P. Gabriel, K. Boubekeur, S. Uriel, P. Batail, *Chem. Rev.* **2001**, *101*, 2037–2066; e) H. D. Selby, B. K. Roland, Z. P. Zheng, *Acc. Chem. Res.* **2003**, *36*, 933–944.

[11] a) E. G. Tulsky, N. R. M. Crawford, S. A. Baudron, P. Batail, J. R. Long, *J. Am. Chem. Soc.* **2003**, *125*, 15543–15553; b) D. H. Johnston, C. L. Stern, D. F. Shriver, *Inorg. Chem.* **1993**, *32*, 5170–5175; c) N. Prokopuk, D. F. Shriver, *Inorg. Chem.* **1997**, *36*, 5609–5613; d) Y. V. Mironov, V. E. Fedorov, I. Ijjaali, J. A. Ibers, *Inorg. Chem.* **2001**, *40*, 6320–6323; e) A. Itasaka, M. Abe, T. Yoshimura, K. Tsuge, M. Suzuki, T. Imamura, Y. Sasaki, *Angew. Chem. Int. Ed.* **2002**, *41*, 463–466.

[12] a) S. Jin, F. J. DiSalvo, *Chem. Mater.* **2002**, *14*, 3448–3457; b) L. G. Beauvais, M. P. Shores, J. R. Long, *Chem. Mater.* **1998**, *10*, 3783–3786; c) N. G. Naumov, A. V. Virovets, M. N. Sokolov, S. B. Artemkina, V. E. Federov, *Angew. Chem. Int. Ed.* **1998**, *37*, 1943–1945; d) M. V. Bennett, M. P. Shores, L. G. Beauvais, J. R. Long, *J. Am. Chem. Soc.* **2000**, *122*, 6664–6668; e) S. B. Artemkina, N. G. Naumov, A. V. Virovets, V. E. Federov, *Eur. J. Inorg. Chem.* **2005**, 142–146; f) Y. V. Mironov, N. G. Naumov, K. A. Brylev, O. A. Efremova, V. E. Fedorov, K. Hegetschweiler, *Angew. Chem. Int. Ed.* **2004**, *43*, 1297–1300.

[13] a) B. B. Yan, H. J. Zhou, A. Lachgar, *Inorg. Chem.* **2003**, *42*, 8818–8822; b) N. G. Naumov, D. V. Soldatov, J. A. Ripmeester, S. B. Artemkina, V. E. Federov, *Chem. Commun.* **2001**, 571–572; c) L. G. Beauvais, M. P. Shores, J. R. Long, *J. Am. Chem. Soc.* **2000**, *122*, 2763–2772; d) M. P. Shores, L. G. Beauvais, J. R. Long, *Inorg. Chem.* **1999**, *38*, 1648–1649; e) M. V. Bennett, L. G. Beauvais, M. P. Shores, J. R. Long, *J. Am. Chem. Soc.* **2001**, *123*, 8022–8032; f) N. G. Naumov, S. Cordier, C. Perrin, *Solid State Sci.* **2005**, *7*, 1517–1521.

[14] H. J. Zhou, C. S. Day, A. Lachgar, *Chem. Mater.* **2004**, *16*, 4870–4877.

[15] a) H. J. Zhou, C. S. Day, A. Lachgar, *Cryst. Growth Des.* **2006**, *6*, 2384–2391; b) H. J. Zhou, K. C. Strates, M. A. Munoz, K. J. Little, D. M. Pajerowski, M. W. Meisel, T. A. Talham, A. Lachgar, *Chem. Mater.* **2007**, *19*, 2238–2246; c) J. J. Zhang, A. Lachgar, *J. Am. Chem. Soc.* **2007**, *129*, 250–251; d) J. J. Zhang, H. J. Zhou, A. Lachgar, *Angew. Chem. Int. Ed.* **2007**, *46*, 4995–4998; e) J. J. Zhang, Y. Zhao, S. A. Gamboa, A. Lachgar, *Cryst. Growth Des.* **2008**, *8*, 172–175.

[16] a) Y. Kim, S.-M. Park, W. Nam, S.-J. Kim, *Chem. Commun.* **2001**, 1470–1471; b) Y. Kim, S.-M. Park, W. Nam, S.-J. Kim, *Inorg. Chem. Commun.* **2002**, *5*, 592–595.

[17] A. Panja, N. Shaikh, M. Ali, P. Vojtisek, P. Banerjee, *Polyhedron* **2003**, *22*, 1191–1198.

[18] H. Miyasaka, H. Ieda, N. Matsumoto, K. Sugiura, M. Yamashita, *Inorg. Chem.* **2003**, *42*, 3509–3515.

 © 2008 Wiley-VCH Verlag GmbH & Co. KGaA, Weinheim

[19] a) S. Demeshko, S. Dechert, F. Meyer, *J. Am. Chem. Soc.* **2004**, *126*, 4508–4509; b) M. Mascal, I. Yakovlev, E. B. Nikitin, J. C. Fettinger, *Angew. Chem. Int. Ed.* **2007**, *46*, 8782–8784; c) O. B. Berryman, V. S. Bryantsev, D. P. Stay, D. W. Johnson, B. P. Hay, *J. Am. Chem. Soc.* **2007**, *129*, 48–58.
[20] a) S. Saha, D. Mal, S. Koner, A. Bhattacherjee, P. Gutlich, S. Mondal, M. Mukherjee, K.-I. Okamoto, *Polyhedron* **2004**, *23*, 1811–1817; b) H. Miyasaka, R. Clérac, T. Ishii, H. C. Chang, S. Kitagawa, M. Yamashita, *J. Chem. Soc., Dalton Trans.* **2002**, 1528–1534 and references cited therein; c) Z. L. Lu, M. Yuan, F. Pan, S. Gao, D. Q. Zhang, D. B. Zhu, *Inorg. Chem.* **2006**, *45*, 3538–3548.
[21] A. L. Spek, *PLATON*, Version 1.62, University of Utrecht, **1999**.
[22] Y. F. Peng, H. Y. Ge, B. Z. Li, B. L. Li, Y. Zhang, *Cryst. Growth Des.* **2006**, *6*, 994–998.
[23] M. Sarkar, K. Biradha, *Cryst. Growth Des.* **2006**, *6*, 1742–1745.
[24] a) K. Biradha, Y. Hongo, M. Fujita, *Angew. Chem. Int. Ed.* **2002**, *41*, 3395–3398; b) K. Uemura, S. Kitagawa, M. Kondo, K. Fukui, R. Kitaura, H. C. Chang, T. Mizutani, *Chem. Eur. J.* **2002**, *8*, 3586–3600.
[25] R. Custelcean, B. A. Moyer, *Eur. J. Inorg. Chem.* **2007**, 1321–1340.
[26] H. Li, Z. J. Zhong, C. Duan, X. You, T. C. W. Mak, B. Wu, *J. Coord. Chem.* **1997**, *41*, 183–189.
[27] GADDS V4.1.14 "*General Area Detector Diffraction System Program for Instrument Control and zData Collection*" Bruker AXS Inc., 5465 East Cheryl Parkway, Madison, WI 53711–5373 USA.
[28] EVA V8.0 "*Graphics Program for 2-dimensional Data evaluation and Presentation*" Bruker AXS Inc., 5465 East Cheryl Parkway, Madison, WI 53711–5373 USA.

Received: January 29, 2008
Published Online: May 28, 2008

 © 2008 Wiley-VCH Verlag GmbH & Co. KGaA, Weinheim